J|A|C|S

ARTICLES

Highly Efficient Solar Cell Polymers Developed via Fine-Tuning of Structural and Electronic Properties

Yongye Liang,[†] Danqin Feng,[†] Yue Wu,[‡] Szu-Ting Tsai,[‡] Gang Li,*,[‡] Claire Ray,[†] and Luping Yu*,[†]

Department of Chemistry and the James Franck Institute, The University of Chicago, 929 E. 57th Street, Chicago, Illinois 60637, and Solarmer Energy Inc., 3445 Fletcher Avenue, El Monte, California 91731

Received February 27, 2009; E-mail: lupingyu@uchicago.edu; gangl@solarmer.com

Abstract: This paper describes synthesis and photovoltaic studies of a series of new semiconducting polymers with alternating thieno[3,4-*b*]thiophene and benzodithiophene units. The physical properties of these polymers were finely tuned to optimize their photovoltaic effect. The substitution of alkoxy side chains to the less electron-donating alkyl chains or introduction of electron-withdrawing fluorine into the polymer backbone reduced the HOMO energy levels of polymers. The structural modifications optimized polymers' spectral coverage of absorption and their hole mobility, as well as miscibility with fulleride, and enhanced polymer solar cell performances. The open circuit voltage, V_{oc}, for polymer solar cells was increased by adjusting polymer energy levels. It was found that films with finely distributed polymer/fulleride interpenetrating network exhibited improved solar cell conversion efficiency. Efficiency over 6% has been achieved in simple solar cells based on fluorinated **PTB4**/$PC_{61}BM$ films prepared from mixed solvents. The results proved that polymer solar cells have a bright future.

Introduction

Semiconducting polymers have shown physical properties similar to those of typical inorganic semiconductors, although the underlying mechanisms are usually different from each other.[1] Photovoltaic effect is one of these properties that stimulate people's enthusiasm because solar energy conversion into electricity is the cleanest way to harvest this vast renewable energy source. So far, the most efficient architecture to build polymeric photovoltaic solar cells is the bulk heterojunction (BHJ) structure prepared by mixing electron-rich polymers and electron-deficient fullerides.[2] This approach can be easily implemented and allows a quick survey of the best composition of polymeric active films. Detailed studies by many groups in the past years have identified poly(3-hexylthiophene) (P3HT) as the most attractive donor material. Power conversion efficiency (PCE) of about 5% has been achieved in solar cells based on P3HT/[6,6]-phenyl-C_{61}-butyric acid methyl ester ($PC_{61}BM$) derivatives.[3] Although it is significant progress in a relatively short period of research time, it is still far away from commercial viability.[4] After an exhaustive research effort, it becomes increasingly apparent that the PCE of solar cells based on P3HT/$PC_{61}BM$ is approaching its limit. New materials exhibiting better performance are needed in order to achieve the desired performance in these types of solar cells for practical application.[5]

The performance of polymer solar cells is characterized by three parameters: open-circuit voltage (V_{oc}), short-circuit current density (J_{sc}), and fill-factor (FF), all of which are related to the PCE by the following equation: PCE = ($V_{oc} \times J_{sc} \times$ FF)/($I_p \times M$), where I_p is the power density of the incident light irradiation and M is spectral mismatch factor. It has been realized that the ideal polymer in BHJ structure should exhibit a broad absorption with high coefficient in the solar spectrum, high hole mobility, suitable energy level matching to fulleride, and appropriate compatibility with fulleride to form bicontinuous interpenetrating network on a nanoscale.[6] It is difficult to design a polymer to fulfill all these requirements. Current polymer solar cells often suffer from small values in some or all of these parameters due to a variety of issues related to the nature of materials and device engineering. So far, besides the P3HT system, there are very few polymer solar cell systems reported which exceed 5% in power conversion efficiency.[7]

† The University of Chicago.
‡ Solarmer Energy Inc.
(1) Skotheim, T. A.; Reynolds J. *Handbook of conducting polymers*; CRC: London, 2007.
(2) (a) Yu, G.; Gao, J.; Hummelen, J. C.; Wudl, F.; Heeger, A. J. *Science* **1995**, *270*, 1789. (b) Gnes, S.; Neugebauer, H.; Sariciftci, N. S. *Chem. Rev.* **2007**, *107*, 1324.

(3) (a) Li, G.; Shrotriya, V.; Huang, J. S.; Yao, Y.; Moriarty, T.; Emery, K.; Yang, Y. *Nat. Mater.* **2005**, *4*, 864. (b) Ma, W. L.; Yang, C. Y.; Gong, X.; Lee, K. H.; Heeger, A. J. *Adv. Funct. Mater.* **2005**, *15*, 1617. (c) Li, G.; Shrotriya, V.; Yao, Y.; Yang, Y. *J. Appl. Phys.* **2005**, *98*, 043704.
(4) Scharber, M.; Muhlbacher, D.; Koppe, M.; Denk, P.; Waldauf, C.; Heeger, A. J.; Brabec, C. *Adv. Mater.* **2006**, *18*, 789.
(5) Thompson, B. C.; Frechet, J. M. J. *Angew. Chem., Int. Ed.* **2008**, *47*, 58.
(6) Roncali, J. *Macromol. Rapid Commun.* **2007**, *28*, 1761.
(7) (a) Muhlbacher, D.; Scharber, M.; Morana, M.; Zhu, Z. G.; Waller, D.; Gaudiana, R.; Brabec, C. *Adv. Mater.* **2006**, *18*, 2884. (b) Peet, J.; Kim, J. Y.; Coates, N. E.; Ma, W. L.; Moses, D.; Heeger, A. J.; Bazan, G. C. *Nat. Mater.* **2007**, *6*, 497. (c) Wang, E. G; Wang, L.; Lan, L. F.; Luo, C.; Zhuang, W. L.; Peng, J. B.; Cao, Y. *Appl. Phys. Lett.* **2008**, *92*, 33307. (d) Hou, J. H.; Chen, H. Y.; Zhang, S. Q.; Li, G.; Yang, Y. *J. Am. Chem. Soc.* **2008**, *130*, 16144.
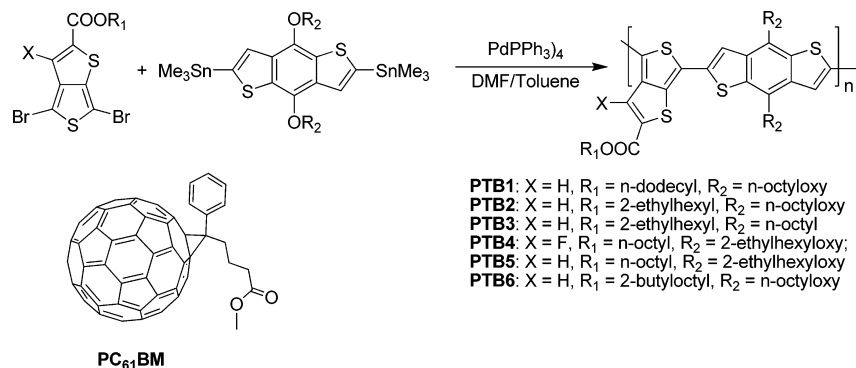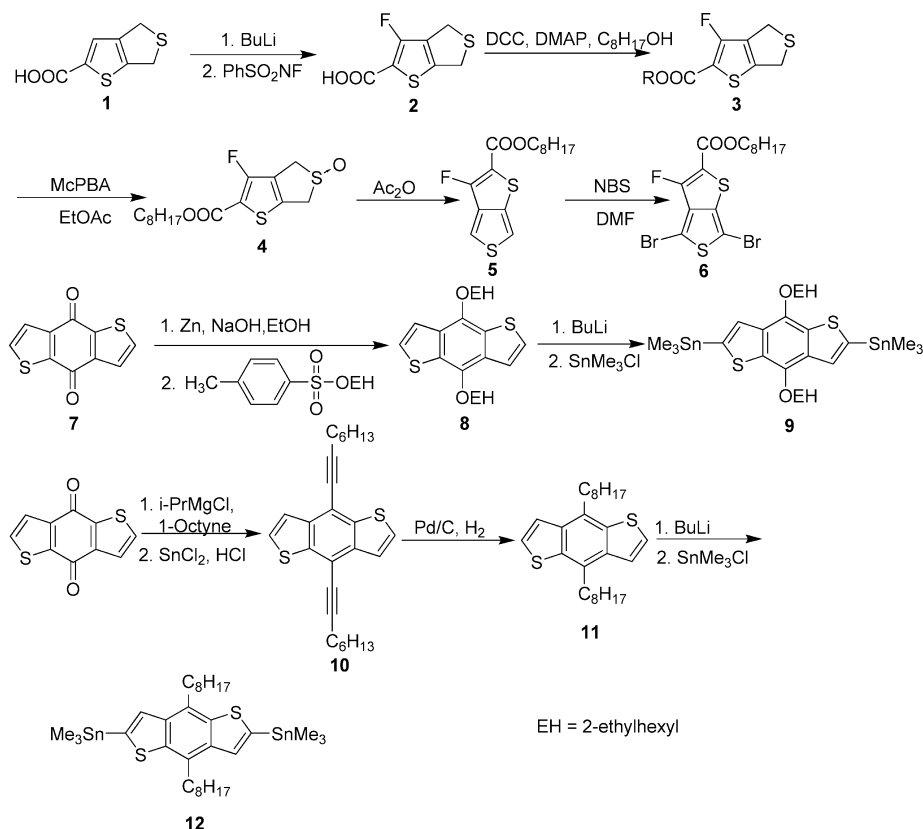
Figure 1. Synthetic routes for polymers **PTB1**−**PTB6** and structure of PC$_{61}$BM.

Scheme 1. Synthesis Routes for Monomers

Recently, we have developed a new polymer, namely **PTB1,** based on alternating thieno[3,4-*b*]thiophene and benzodithiophene units (Figure 1). Simple single-layer polymer solar cells exhibited solar conversion efficiency of 4.8% based on **PTB1**/PC$_{61}$BM BHJ structure and 5.6% on **PTB1**/PC$_{71}$BM structure.[8] The J_{sc} and FF obtained from such polymer solar cells are among the highest values reported for solar cell system based on low-band-gap polymers. However, the V_{oc} of the polymer solar cells is relatively small, just about 0.56−0.58 V. In this paper, we describe our results in the development of new polymers which exhibit higher solar cell conversion efficiencies. These polymers were developed via synthetic fine-tuning of their structural and electronic properties.

Experimental Section

Materials. Otherwise stated, all of the chemicals are purchased from Aldrich and used as received. The 4,6-dihydrothieno[3,4-*b*]thiophene-2-carboxylic acid (**1**),[9] 4,6-dibromothieno[3,4-*b*]thiophene-2-carboxylic esters,[8] 1,5-bis(trimethyltin)-4,8-dioctylbenzo[1,2-*b*:4,5-*b*']dithiophene,[7] and benzo[1,2-b:4,5-*b*′*b*′]dithiophene-4,8-dione[10] were synthesized according to the procedures reported in the literature. Other monomers were synthesized according to Scheme 1.

3-Fluoro-4,6-dihydrothieno[3,4-*b*]thiophene-2-carboxylic acid (2). The 4,6-dihydrothieno[3,4-*b*]thiophene-2-carboxylic acid (1.46 g, 7.85 mmol) was dissolved in 60 mL of THF and cooled in an acetone/dry ice bath under nitrogen protection. Butyllithium solution ((6.9 mL, 17.3 mmol) was added dropwise with stirring. The

(8) Liang, Y. Y.; Wu, Y.; Feng, D. Q.; Tsai, S. T.; Son, H. J.; Li, G.; Yu, L. P. *J. Am. Chem. Soc.* **2009**, *131*, 56.

(9) Yao, Y.; Liang, Y. Y.; Shrotriya, V.; Xiao, S. Q.; Yu, L. P.; Yang, Y. *Adv. Mater.* **2007**, *19*, 3979.

(10) Beimling, P; Koβmehl, G. *Chem. Ber.* **1986**, *119*, 3198.

resulting mixture was kept in a dry ice bath for 1 h. Then *N*-fluorobenzenesulfonimide (3.22 g, 10.2 mmol) in 20 mL of THF was added dropwise, and the solution was stirred at RT overnight. The reaction was quenched with 50 mL of water, and the organic solvent was removed by evaporation at reduced pressure. The solid residue was collected by filtration and purified by chromatography on silica with ethyl acetate. A mixture of 1.30 g containing fluorinated product and unfluorinated reactant with a 4:1 ratio was obtained. The calculated mass of fluorinated product is 1.04 g, 65%. ^{1}HNMR (D_6-DMSO): δ 4.01−4.05 (2H, t, $J = 3$ Hz), 4.20−4.24 (2H, t, $J = 3$ Hz). MS (EI): Calcd, 204.0; found $(M − 1)^-$, 202.9.

Octyl 3-Fluoro-4,6-dihydrothieno[3,4-*b*]thiophene-2-carboxylate (3). The raw materials of **2** (1.30 g, 6.3 mmol), DCC (1.58 g), and DMAP (260 mg) were added to a 50 mL round-bottom flask with CH_2Cl_2 (15 mL). 1-Octanol (8.22 g, 63 mmol) was added to the flask and then stirred for 20 h under N_2 protection. The reaction mixture was poured to 100 mL of water and extracted with CH_2Cl_2. The organic phase was dried by sodium sulfate, and the solvent was removed. Column chromatography on silica gel using hexane/ $CH_2Cl_2 = 1/1$ yielded the title compound as an oil (1.42 g, 71%). ^{1}HNMR (CDCl$_3$): δ 0.85−0.91 (3H, t, $J = 6$ Hz), 1.22−1.45 (10H, m), 1.68−1.76 (2H, m), 3.99−4.02 (2H, t, $J = 3$ Hz), 4.15−4.18 (2H, t, $J = 3$ Hz), 4.24−4.29 (2H, t, $J = 6$ Hz). MS (EI): Calcd, 316.1; found $(M + 1)^+$, 317.0.

Octyl 3-Fluorothieno[3,4-*b*]thiophene-2-carboxylate (5). A solution of compound **3** (1.42 g, 4.5 mmol)) in 100 mL of ethyl acetate was stirred and cooled in a dry ice bath. MCPBA (0.78 g, 4.5 mmol) in 30 mL of ethyl acetate was added dropwise to the reaction solution. The resulting mixture was stirred overnight. The solvent was removed by evaporation, and the residue contained a crude product of **4** and 3-chlorobenzoic acid. The residue was refluxed in acetic anhydride for 2.5 h. The mixture was cooled, and the solvent was removed by evaporation. The residue was purified by flash chromatography on silica gel with hexanes/ dichloromethane (2:1) to give compound **5** (0.95 g, 67%). ^{1}HNMR (CDCl$_3$): 0.85−0.92 (3H, t, $J = 7$ Hz), 1.23−1.48 (10H, m), 1.70−1.80 (2H, m), 4.30−4.35 (2H, t, $J = 7$ Hz), 7.27−7.29 (1H, d, $J = 3$ Hz), 7.65−7.67 (1H, d, $J = 3$ Hz).

Octyl 4,6-Dibromo-3-fluorothieno[3,4-*b*]thiophene-2-carboxylate (6). To a solution of compound **5** (0.95 g, 3.0 mmol) in 10 mL of DMF was added dropwise a solution of NBS (1.34 g, 7.56 mmol) in 10 mL of DMF under nitrogen protection in the dark. The reaction mixture was stirred at RT for 24 h. Then it was poured into saturated sodium sulfite solution in an ice−water bath and extracted with dichloromethane. The organic phase was collected and dried by sodium sulfate. Removal of the solvent and column purification on silica get using dichloromethane/hexane (1/4) yielded the target product (0.98 g, 69%) as a light yellow solid. ^{1}HNMR (CDCl$_3$): 0.85−0.92 (3H, t, $J = 7$ Hz), 1.23−1.48 (10H, m), 1.70−1.80 (2H, m), 4.30−4.35 (2H, t, $J = 7$ Hz). MS (EI): Calcd, 469.9; found $(M + 1)^+$, 471.9.

4,8-Bis(2-ethylhexyloxy)benzo[1,2-*b*:4,5-*b'*]dithiophene (8). The benzo[1,2-*b*:4,5-*b'*]dithiophene-4,8-dione (1.0 g, 4.5 mmol) was mixed with zinc dust (0.65 g, 10 mmol) in a flask. Ethanol (4 mL) and NaOH solution (15 mL, 20%) were added, and the mixture was refluxed for 1 h. 2-Ethylhexyl *p*-toluenesulfonate (4.3 mL) was added in portions with stirring until the color changed to red. The resulting precipitate was filtered; the filtrate was diluted with 100 mL of water and extracted with chloroform (100 mL). The organic extraction was dried with anhydrous sodium sulfate and evaporated in vacuo. Column chromatography on silica gel using dichloromethane and hexanes mixed eluents yielded the compound **8** as a light yellow oil (0.80 g, 40%). ^{1}HNMR (CDCl$_3$): δ0.72−0.90 (12H, m), 1.10−1.38 (16H, m), 1.50−1.62 (2H, m), 3.84−3.97 (4H, m), 7.32−7.36 (2H, d, $J = 5$ Hz), 7.46−7.50 (2H, d, $J = 5$ Hz). MS (EI): Calcd, 446.2; found $(M + 1)^+$, 447.2.

2,6-Bis(trimethyltin)-4,8-bis(2-ethylhexyloxy)benzo[1,2-*b*:4,5-*b'*] dithiophene (9). Compound **8** (0.62 g, 1.4 mmol) was dissolved in 20 mL of anhydrous THF and cooled in an acetone/dry ice bath under

nitrogen protection. Butyllithium solution (1.4 mL, 3.5 mmol) was added dropwise with stirring, after the addition the mixture was kept in a dry ice bath for 30 min and at RT for 30 min. The mixture was cooled in the dry ice bath and trimethyltin chloride solution (4.2 mL, 4.2 mmol, 1 M in hexane) was added, and the mixture was stirred at RT overnight. The mixture was quenched with 50 mL of water and extracted with hexanes. The organic extraction was dried with anhydrous sodium sulfate and evaporated in vacuo. Recrystallization of the residue from isopropanol yield the compound **9** as colorless needles (0.8670 g, 80%). ^{1}HNMR (CDCl$_3$): δ 0.43 (18H, s), 0.90−1.10 (12H, m), 1.33−1.85 (18H, m), 1.54−1.58 (4H, m), 4.15−4.23 (4H, d, $J = 5$ Hz), 7.51 (2H, s).

4,8-Dioctynbenzo[1,2-*b*:4,5-*b'*]dithiophene (10). Isopropylmag-nesium chloride (2 M solution, 12 mL, 24 mmol) was added dropwise to a solution of 1-octyne (2.97 g, 27 mmol) at RT. The reaction mixture was heated up to 60 °C and stirred for 100 min. It was cooled to RT, and benzo[1,2-*b*:4,5-*b'*]dithiophene-4,8-dione (1 g, 4.53 mmol) was added. The reaction mixture was heated up to 60 °C and kept for 60 min. It was then cooled to RT, and 7 g of SnCl$_2$ in HCl solution (16 mL 10%) was added dropwise to the reaction mixture. The reaction mixture was heated at 65 °C for 60 min, then cooled down to room temperature, and poured into 100 mL of water. It was extracted with 50 mL of hexanes twice. The organic phase was combined and dried with anhydrous Na$_2$SO$_4$, and the organic solvent was removed by vacuum evaporation. The residue was purified by column chromatography on silica with hexanes/dichloromethane (3/1, volume ratio), yielding compound **10** (1.66 g, 90%). ^{1}HNMR (CDCl$_3$): δ 0.88−0.96 (6H, t, $J = 5$ Hz), 1.32−1.42 (8H, m), 1.53−1.63 (4H, m), 1.68−1.77 (4H, m), 2.61−2.66 (4H, t, $J = 7$ Hz), 7.48−7.51 (2H, d, $J = 6$ Hz), 7.56−7.58 (2H, d, $J = 6$ Hz). MS (EI): Calcd, 406.2; found $(M + 1)^+$, 407.1.

4,8-Dioctylbenzo[1,2-*b*:4,5-*b'*]dithiophene (11). To the solution of compound **2** (1.66 g, 4.07 mmol) in 75 mL of THF was added Pd/C (0.45 g, 10%), and the reaction mixture was kept in a hydrogen atmosphere for 18 h at RT. The mixture was filtered with Celite, and the solvent was removed by vacuum evaporation. The residue was purified by column chromatography on silica with hexane as the eluent, yielding compound **11** (0. 95 g, 56%) as white solids. ^{1}HNMR (CDCl$_3$): δ 0.85−0.92 (6H, t, $J = 7$ Hz), 1.20−1.40 (16H, m), 1.40−1.50 (4H, m), 1.76−1.84 (4H, m), 3.13−3.21 (4H, t, $J = 8$ Hz), 7.43−7.45 (2H, d, $J = 6$ Hz), 7.46−7.48 (2H, d, $J = 6$ Hz). MS (EI): Calcd, 414.2; found $(M + 1)^+$, 415.2.

2,6-Bis(trimethyltin)-4,8-dioctylbenzo[1,2-*b*:4,5-*b'*]dithiophene (12). Compound **3** (0.95 g,2.3 mmol) was dissolved in 20 mL of anhydrous THF and cooled in an acetone/dry ice bath under nitrogen protection. Butyllithium solution (2.3 mL, 5.7 mmol) was added dropwise with stirring. The mixture was kept in a dry ice bath for 30 min and then at RT for 30 min. The mixture was cooled in the dry ice bath, and 6.5 mL (6.5 mmol) of trimethyltin chloride solution (1 M in hexane) was added and stirred at RT for overnight. The mixture was quenched with 50 mL of water and extracted with hexanes. The organic extraction was dried with anhydrous sodium sulfate and evaporated in vacuo. Recrystallization of the residue from isopropanol yields the titled compound **12** (0.50 g, 88%). ^{1}HNMR (CDCl$_3$): δ 0.45 (18H, s), 0.87−0.91 (6H, t, $J = 7$ Hz), 1.25 −1.42 (16H, m), 1.42−1.51 (4H, m), 1.76−1.85 (4H, m), 3.17−3.23 (4H, t, $J = 8$ Hz), 7.49 (2H, s).

Synthesis of Polymers. PTB4. Octyl-6-dibromo-3-fluo-rothieno[3,4-*b*]thiophene-2-carboxylate (**6**) (236 mg, 0.50 mmol) was weighted into a 25 mL round-bottom flask. 2,6-Bis(trim-ethyltin)-4,8-bis(2-ethylhexyloxy)benzo[1,2-*b*:4,5-*b'*]dithiophe-ne (**9**) (386 mg, 0.50 mmol) and Pd(PPh$_3$)$_4$ (25 mg) were added. The flask was subjected to three successive cycles of vacuum followed by refilling with argon. Then, anhydrous DMF (2 mL) and anhydrous toluene (8 mL) were added via a syringe. The polymerization was carried out at 120 °C for 12 h under nitrogen protection. The raw product was precipitated into methanol and collected by filtration. The precipitate was dissolved in chloro-

form and filtered with Celite to remove the metal catalyst. The final polymers were obtained by precipitating in hexanes and drying in vacuum for 12 h, yielding PTB4 (309 mg, 82%). ^{1}HNMR (CDCl$_2$CDCl$_2$): δ 0.80−2.40 (45H, br), 3.90−4.70 (6H, br), 7.00−7.90 (2H, br). GPC: M_w (19.3 × 10^3 g/mol), PDI (1.32).

PTB2, PTB3, PTB5, and PTB6 are synthesized according to the same procedure as PTB4 with respective monomers. The ^{1}HNMR and gel permeation chromatography (GPC) data of the polymers are listed below.

PTB2. ^{1}HNMR (CDCl$_2$CDCl$_2$): δ 0.70−2.42 (45H, br), 3.90−4.80 (6H, br), 6.70−8.00 (3H, br). GPC: M_w (23.2 × 10^3 g/mol), PDI (1.38).

PTB3. ^{1}HNMR (CDCl$_2$CDCl$_2$): δ 0.70−2.35 (45H, br), 2.90−3.40 (4H, br), 4.20−4.70 (2H, br), 6.70−8.20 (3H, br). GPC: M_w (23.7 × 10^3 g/mol), PDI (1.49).

PTB5. ^{1}HNMR (CDCl$_2$CDCl$_2$): δ 0.90−2.40 (45H, br), 3.90−4.70 (6H, br), 7.00−7.60 (2H, br), 7.60−8.10 (1H, br). GPC: M_w (22.7 × 10^3 g/mol), PDI (1.41).

PTB6. ^{1}HNMR (CDCl$_2$CDCl$_2$): δ 0.70−2.42 (53H, br), 3.90−4.80 (6H, br), 6.70−8.00 (3H, br). GPC: M_w (25.0 × 10^3 g/mol), PDI (1.50).

Characterization. ^{1}H NMR spectra were recorded at 400 or 500 MHz on Bruker DRX-400 or DRX-500 spectrometers, respectively. Molecular weights and distributions of polymers were determined by using GPC with a Waters Associates liquid chromatograph equipped with a Waters 510 HPLC pump, a Waters 410 differential refractometer, and a Waters 486 tunable absorbance detector. THF was used as the eluent and polystyrene as the standard. The optical absorption spectra were taken by a Hewlett-Packard 8453 UV−vis spectrometer.

Cyclic voltammetry (CV) was used to study the electrochemical properties of the polymers. For calibration, the redox potential of ferrocene/ferrocenium (Fc/Fc$^+$) was measured under the same conditions, and it is located at 0.09 V to the Ag/Ag$^+$ electrode. It is assumed that the redox potential of Fc/Fc$^+$ has an absolute energy level of −4.80 eV to vacuum.[11] The energy levels of the highest (HOMO) and lowest unoccupied molecular orbital (LUMO) were then calculated according to the following equations

$$E_{HOMO} = -(\phi_{ox} + 4.71)\ (eV)$$

$$E_{LUMO} = -(\phi_{red} + 4.71)\ (eV)$$

where ϕ_{ox} is the onset oxidation potential vs Ag/Ag$^+$ and ϕ_{red} is the onset reduction potential vs Ag/Ag$^+$.

Hole mobility was measured according to a similar method described in the literature,[12] using a diode configuration of ITO/poly(ethylenedioxythiophene) doped with poly(styrenesulfonate) (PEDOT:PSS)/polymer/Al by taking current−voltage current in the range of 0−6 V and fitting the results to a space charge limited form, where the SCLC is described by

$$J = 9\varepsilon_0\varepsilon_r\mu V^2/8L^3$$

where ε_0 is the permittivity of free space, ε_r is the dielectric constant of the polymer, μ is the hole mobility, V is the voltage drop across the device, L is the polymer thickness, and $V = V_{appl} - V_r - V_{bi}$, where V_{appl} is the applied voltage to the device, V_r is the voltage drop due to contact resistance and series resistance across the electrodes, and V_{bi} is the built-in voltage due to the difference in work function of the two electrodes. The resistance of the device was measured using a blank configuration ITO/PEDOT:PSS/Al and

was found to be about 10−20 Ω. The V_{bi} was deduced from the best fit of the $J^{0.5}$ versus V_{appl} plot at voltages above 2.5 V and is found to be about 1.5 V. The dielectric constant, ε_r, is assumed to be 3 in our analysis, which is a typical value for conjugated polymers. The thickness of the polymer films is measured by using AFM.

Device Fabrication. The polymers PTB1−PTB6 were codissolved with PC$_{61}$BM in 1,2-dichlorobenzene (DCB) in the weight ratio of 1:1, respectively. PTB1, PTB2, and PTB6 concentrations are 10 mg/mL, while PTB3, PTB4, and PTB5 concentrations are 13 mg/mL. For the last three polymer solutions, we also studied mixed solvent effect with about 3% (volume) 1,8-diiodooctane, also used to further improve the final device performances.

ITO-coated glass substrates (15Ω/□) were cleaned stepwise in detergent, water, acetone, and isopropyl alcohol under ultrasonication for 15 min each and subsequently dried in an oven for 5 h. A thin layer (∼30 nm) of PEDOT:PSS (Baytron P VP A1 4083) was spin-coated onto ITO surface which was pretreated by ultraviolet ozone for 15 min. Low-conductivity PEDOT:PSS was chosen to minimize measurement error from device area due to lateral conductivity of PEDOT:PSS. After being baked at 120 °C for ∼20 min, the substrates were transferred into a nitrogen-filled glovebox (<0.1 ppm O$_2$ and H$_2$O). A polymer/PCBM composites layer (ca.100 nm thick) was then spin-cast from the blend solutions at 1000 rpm on the ITO/PEDOT:PSS substrate without further special treatments. Then the film was transferred into a thermal evaporator which is located in the same glovebox. A Ca layer (25 nm) and an Al layer (80 nm) were deposited in sequence under the vacuum of 2 × 10^{-6} torr. The effective area of film was measured to be 0.095 cm^2.

Current−Voltage Measurement. The fabricated device was encapsulated in a nitrogen-filled glovebox by UV epoxy (bought from Epoxy Technology) and cover glass. The current density−voltage (J−V) curves were measured using a Keithley 2400 source-measure unit. The photocurrent was measured under AM 1.5 G illumination at 100 mW/cm^2 under the Newport Thermal Oriel 91192 1000W solar simulator (4 in. × 4 in. beam size). The light intensity was determined by a monosilicon detector (with KG-5 visible color filter) calibrated by National Renewable Energy Laboratory (NREL) to minimize spectral mismatch.

External quantum efficiencies (EQEs) were measured at UCLA by using a lock-in amplifier (SR830, Stanford Research Systems) with current preamplifier (SR570, Stanford Research Systems) under short-circuit conditions. The devices were illuminated by monochromatic light from a xenon lamp passing through a monochromator (SpectraPro-2150i, Acton Research Corporation) with a typical intensity of 10 μW. Prior to incident on the device, the monochromic incident beam is chopped with a mechanical chopper connected to the lock-in amplifier and then focused on the testing pixel of the device. The photocurrent signal is then amplified by SR570 and detected with SR830. A calibrated mono silicon diode with known spectral response is used as a reference.

Conductive Atomic Force Microscopy (CAFM) Measurement. All CAFM measurements were done under ambient conditions using a commercial scanning probe microscope (Asylum Research, MFP-3D). Platinum-coated, contact-mode AFM cantilevers with spring constant of 0.2 N/m and tip radius of ca. 25 nm (Budget Sensors) were used to map out the hole-current of films in the dark using contact mode. The deflection set point is 0.3 V and bias voltage is −2 V for all the sample measurements, and the conditions used to prepare the films are the same to make the solar cell device.

Results and Discussion

Synthesis. The encouraging results of polymer PTB1 lead us to select the polymer backbone as the structural platform to investigate structure/property relationship and to search for new polymers with improved solar cell performance.[8] The PTB1

(11) Pommerehne, J.; Vestweber, H.; Guss, W.; Mahrt, R. F.; Bassler, H.; Porsch, M.; Daub, J. Adv. Mater. 1995, 7, 551.
(12) (a) Malliaras, G. G.; Salem, J. R.; Brock, P. J.; Scott, C. Phys. Rev. B 1998, 58, 13411. (b) Goh, C.; Kline, R. J.; McGehee, M. D.; Kadnikova, E. N.; Frechet, J. M. J. Appl. Phys. Lett. 2005, 86, 122110.
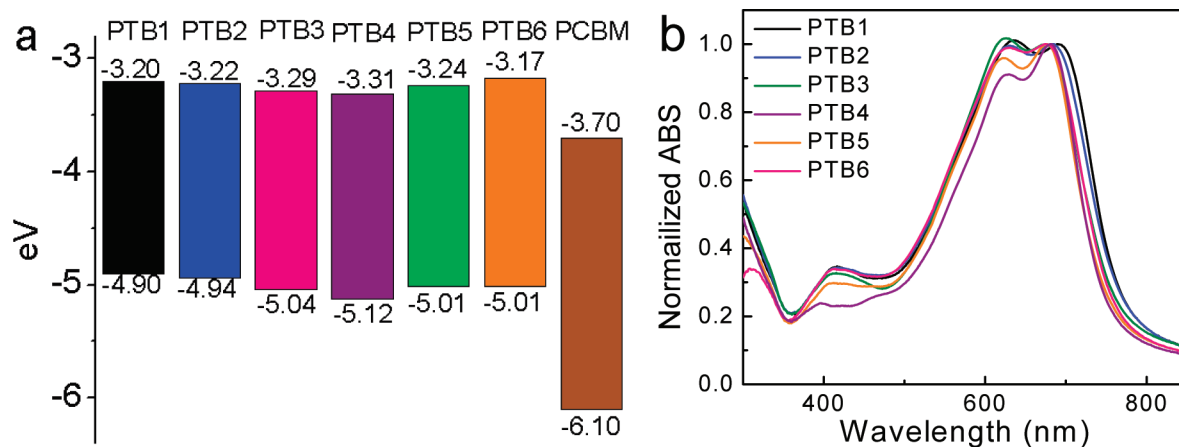
Figure 2. (a) HOMO and LUMO energy levels of the polymers. Energy levels of PC$_{61}$BM are listed for comparison. (b) UV−vis absorption spectra of the polymer films.

was designed based on the concept that the thienothiophene moiety can support the quinoidal structure and lead to narrow polymer band gap, which is crucial to efficiently harvesting solar energy. Since the thienothiophene moiety is very electron-rich, an electron-withdrawing ester group is introduced to stabilize the resulting polymers. Indeed, the results confirmed our design idea.[9] However, we also noticed that the long *n*-dodecyl side chain is grafted on the thieno[3,4-*b*]thiophene ester in **PTB1**, which may decrease the miscibility of the conjugated polymer with PC$_{61}$BM and affect the formation of effective interpenetrating network.[13] The small V_{oc} value indicates the need to adjust the HOMO−LUMO energy level relative to fullerides.[4] With these considerations in mind, we have synthesized six related polymers as shown in Figure 1.

The polymerization was carried out via the Stille polycondensation reaction.[14] The corresponding monomers were synthesized according to Scheme 1. To shorten the dodecyl ester chain in PTB1, an *n*-octyl side chain substituted polymer was synthesized. However, this polymer exhibits poor solubility, which limits its processing ability, and was not studied further. Soluble **PTB2** was synthesized with shortened and branched side chains. For comparison, a bulkier branched side chain, 2-butyloctyl, was used in **PTB6**. The branched side chain can also be grafted to the benzodithiophene, which leads to **PTB5** with two 2-ethylhexyloxy side chains attached to the benzodithiophene ring. The alkoxy groups grafted on benzodithiophene ring are strong electron-donating groups that can raise the HOMO energy level of the polymer.[15] This will lead to the reduction in V_{oc}, detrimental to the performance of polymer solar cells.[4] In order to further adjust the polymer's electronic properties, **PTB3** with less electron-donating alkyl chains in benzodithiophene was synthesized.

To further lower the HOMO level, a second electron-withdrawing group can be introduced to the 3 position of the thieno[3,4-*b*]thiophene ring. Fluorine is a good candidate to functionalize the 3 position because fluorine has a high electronegativity. The size of the fluorine atom is small, which will introduce only small steric hindrance for the configuration

and packing of the polymer.[16] The fluorinated thieno[3,4-*b*] thiophene was synthesized via a modified route previously reported for ester-substituted thieno[3,4-b]thiophene (Scheme 1).[9] The fluorine was introduced to the fused ring unit from 4,6-dihydrothieno[3,4-*b*]thiophene-2-carboxylic acid after deprotonation by using BuLi and reacting with PhSO$_2$NF. The fluorinated acid was first converted to ester and then dibromo-substituted thieno[3,4-*b*]thiophene. Initially, we attempted to introduce fluorine atom to **PTB1** (R_1 = *n*-dodecyl, R_2 = *n*-octyloxy). The obtained polymer exhibited poor solubility and only dissolves in dichlorobenzene over 100 °C, which makes it difficult to prepare uniform films. To increase the solubility, benzodithiophene substituted with branch side chains was used, and the fluorinated polymer, **PTB4**, was obtained.

The structures of polymers were characterized with ^{1}HNMR spectroscopy, all consistent with the proposed ones. Gel permeation chromatography (GPC) studies showed that these polymers have similar weight-averaged molecular weights between 19.3 and 25.0 kg/mol with a relatively narrow polydispersity index (PDI) between 1.25 and 1.50. The results indicate that the changes in monomer structures did not lead to significant changes in polymerization reaction. These polymers have good solubility in chlorinated solvents, such as chloroform and chlorobenzene. Thermogravimetric analyses (TGA) indicate that the polymers are stable up to about 200 °C.

Electrochemical and Optical Properties. The HOMO and LUMO energy levels of the polymers were determined by cyclic voltammetry (CV), and the results are summarized in Figure 2a. The HOMO energy levels of the polymers are very close except for **PTB3** and **PTB4**. From the comparison of **PTB2** and **PTB3**, it was noticed that the substitution of octyloxy side chain to octyl side chain lowered the HOMO energy level of the polymer from −4.94 to −5.04 eV. Comparing **PTB4** and **PTB5**, polymers with same side chain patterns, it is clear that the introduction of the electron-withdrawing fluorine in the polymer backbone significantly lowered the HOMO level. The film absorption spectra of the polymers are showed in Figure 2b, and characteristics of the polymer absorption are summarized in Table 1. All these polymers show very similar absorption spectra; the changes of the absorption peak and onset point among the polymers are within 25 nm.

(13) Thompson, B. C.; Kim, B. J.; Kavulak, D. F.; Sivula, K.; Mauldin, C.; Frechet, J. M. J. *Macromolecules* **2007**, *40*, 7425.
(14) Bao, Z. N.; Chan, W. K.; Yu, L. P. *J. Am. Chem. Soc.* **1995**, *117*, 12426.
(15) Daoust, G.; Leclerc, M. *Macromolecules* **1991**, *24*, 455.

(16) Babudri, F.; Farinola, G. M.; Naso, F.; Ragni, R. *Chem. Commun.* **2007**, 1003.

Table 1. Molecular Weight and Absorption Properties of the Polymers

polymers	M_w (kg/mol)	PDI	μ_{peak} (nm)	μ_{onset} (nm)	E_g^{opt} (eV)
PTB1	22.9	1.25	687,638	786	1.58
PTB2	23.2	1.38	683,630	780	1.59
PTB3	23.7	1.49	682,628	777	1.60
PTB4	19.3	1.32	682,627	762	1.63
PTB5	22.7	1.41	677,623	764	1.62
PTB6	25.0	1.50	675,630	768	1.61

Hole Mobility. The hole mobility of the polymers is measured according to method based on the space charge limited current (SCLC) model,[12] and the results are plotted in Figure 3. The hole mobilities of 4.7×10^{-4}, 4.0×10^{-4}, 7.1×10^{-4}, 7.7×10^{-4}, 4.0×10^{-4}, and 2.6×10^{-4} cm^2/V·s are found for **PTB1**, **PTB2**, **PTB3**, **PTB4**, **PTB5**, and **PTB6**, respectively. A small decrease of the polymer hole mobility is observed after the introduction of bulky branched side chains to the polymer backbones. It is expected that the bulky side chains may increase the steric hindrance for intermolecular packing, so the hole mobility decreases. This explains that the largest decrease of the hole mobility happens to **PTB6**, which has the bulkiest 2-butyloctyl side chain on the ester group. It is interesting to note that the alkyl-grafted **PTB3** has higher mobility than the alkoxy-grafted **PTB2**, though they both have similar side chain patterns. **PTB4** has the largest hole mobility of 7.7×10^{-4} cm^2/V·s among these polymers. It has been reported that there is a strong π-stacking interaction between the electron-deficient fluorinated aromatic rings and the electron-rich nonfluorinated ones in the fluorine-substituted aromatic moieties.[17] The increase of mobility in fluorinated **PTB4** is probably due to the increase in intermolecular packing between the fluorinated backbone. Detailed studies by using grazing angle X-ray diffraction are in progress to elucidate polymer structures and will be presented in a future publication.

Photovoltaic Properties. Photovoltaic properties of the polymers were investigated in solar cell structures of ITO/PEDOT:PSS/polymer:PC$_{61}$BM(1:1, wt ratio)/Ca/Al. The polymer active layers were spin-coated from a dichlorobenzene solution. Figure 4 shows the photo J–V curves of the polymer solar cells under AM 1.5 condition at 100 mW/cm^2. Representative characteristics of the solar cells are summarized in Table 2. Generally, the bulky side chain grafted polymers show larger V_{oc} than **PTB1**, as they have lower HOMO energy levels. The alkyl-substituted
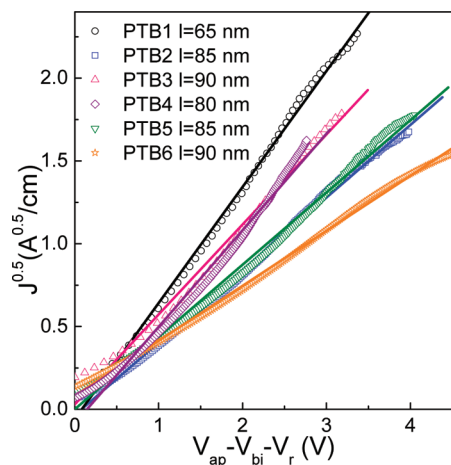
Figure 3. $J^{0.5}$ vs V plots for the polymer films. The solid lines are fits of the data points. The thickness of the films is indicated in the plots.
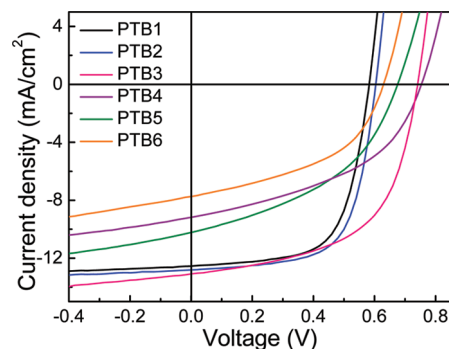
Figure 4. Current–voltage characteristics of polymer/PC$_{61}$BM solar cells under AM 1.5 condition (100 mW/cm^2).

Table 2. Characteristic Properties of Polymer Solar Cells

polymers	V_{oc} (V)	J_{sc} (mA/cm^2)	FF (%)	PCE (%)
PTB1	0.58	12.5	65.4	4.76
PTB2	0.60	12.8	66.3	5.10
PTB3	0.74	13.1	56.8	5.53
PTB4	0.76	9.20	44.5	3.10
PTB5	0.68	10.3	43.1	3.02
PTB6	0.62	7.74	47.0	2.26
PTB3[a]	0.72	13.9	58.5	5.85
PTB4[a]	0.74	13.0	61.4	5.90(6.10[b])
PTB5[a]	0.66	10.7	58.0	4.10

[a] Devices prepared from mixed solvents dichlorobenzene/diiodooctane (97/3, v/v). [b] Value after spectral correction.

PTB3 has an enhanced V_{oc} compared to **PTB2**, which is expected from the HOMO energy level difference. The fluorinated polymer **PTB4** devices showed a larger V_{oc} than **PTB5**. However, except for **PTB2** and **PTB3**, the other polymer solar cells suffer obvious decrease in short-circuit current (J_{sc}) and fill factor (FF) compared to the **PTB1** solar cell. Further studies by using transmission electron microscopy (TEM) indicated that the poor solar cell performances in **PBT3**–**PTB6** are related to the nonoptimized morphology, which has a large effect on the BHJ polymer solar cell performance (Figure 5).[18] The TEM images of **PTB2**/PC$_{61}$BM blend film show finer features comparable to the **PTB1** one, which may be due to the increase in the miscibility of the polymer with PC$_{61}$BM after shortening the dodecyl side chain into the 2-ethylhexyl side chain. As a result, J_{sc} and FF in the **PTB2** solar cell are slightly larger than the **PTB1** one. However, large domains are observed in their PC$_{61}$BM blend films of **PTB5** or **PTB6**. The bulky side chains reduce the miscibility of polymer with PC$_{61}$BM, leading to better phase separation between polymer chains and PC$_{61}$BM molecules. As a result, the interfacial areas of charge separation in **PTB5** or **PTB6** are reduced, and the polymer solar cell performances are diminished. It is not coincident that the **PTB6** has the largest feature sizes (150–200 nm) in the TEM image and its solar cell performance is the worst. With the same side chain patterns as **PTB5**, the fluorinated **PTB4** also suffers the nonoptimized morphology, as shown by the large features (over 100 nm) in the TEM image of **PTB4**/PC$_{61}$BM blend film. Although **PTB4** shows the lowest HOMO energy level and the largest hole mobility, its photovoltaic performance in simple polymer/PC$_{61}$BM solar cells is modest (3.10%). Comparing

(17) Feast, W.; Lovenich, P. W.; puschmann, H.; Taliani, C. *Chem. Commun.* **2001**, 505.
(18) (a) Yang, X. N.; Loos, J. *Macromolecules* **2007**, *40*, 1353. (b) Li, G; Yao, Y.; Yang, H. C.; Shrotriya, V.; Yang, G. W.; Yang, Y. *Adv. Funct. Mater.* **2007**, *17*, 1636.
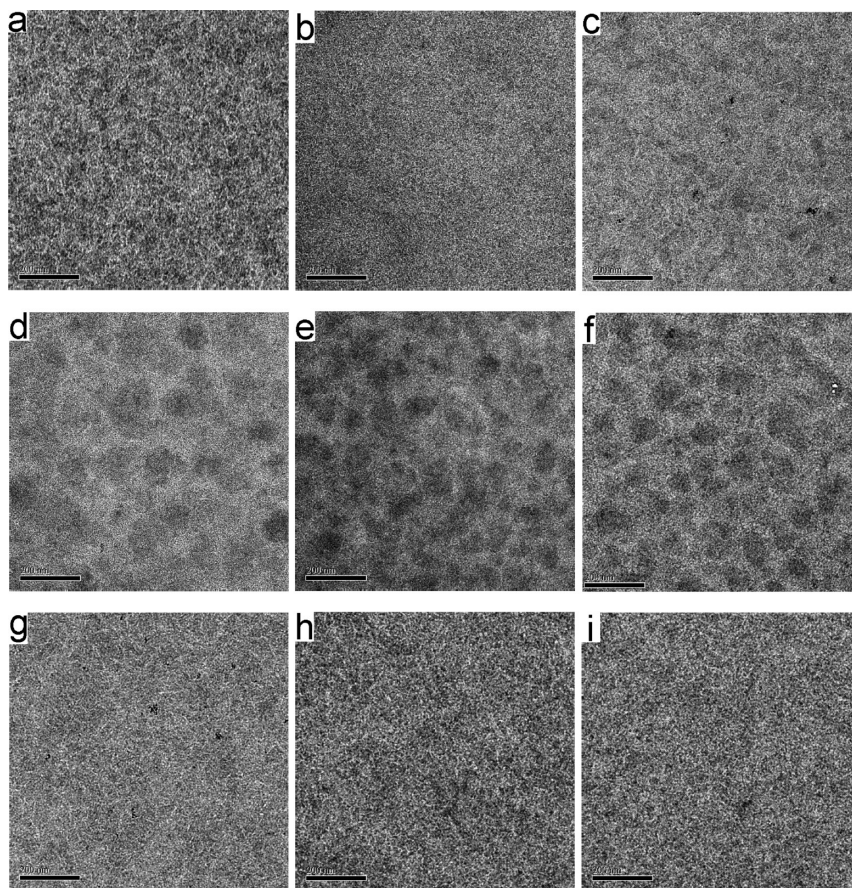
Figure 5. TEM images of polymer/PC$_{61}$BM blend films **PTB1** (a), **PTB2** (b), **PTB3** (c), **PTB4** (d), **PTB5** (e), and **PTB6** (f) and polymer/PC$_{61}$BM blend films prepared from mixed solvents dichlorobenzene/diiodooctane (97/3, v/v) **PTB3** (g), **PTB4** (h), and **PTB5** (i).

PTB2 and **PTB3** with similar side chain patterns, **PTB3** has a larger J_{sc} than **PTB2**, which is due to the increase of hole mobility in **PTB3**. However, the better packing ability in **PTB3** may reduce its miscibility with PC$_{61}$BM, and there are a few large features (about 50 nm) in the TEM images of **PTB3**/PC$_{61}$BM blend film. Due to the nonoptimized morphology, the **PTB3** solar cell suffers a slight decrease in FF compared to **PTB2**. But with the increase in J_{sc} and V_{oc}, the **PTB3** device still shows 5.53% PCE.

Insightful information on the effect of morphology on charge transport behaviors of composite films was obtained from studies using conductive atomic force microscopy (CAFM).[19] The two-dimensional current maps correlate well with nanoscale domain structure observed from TEM in solar cell films. We select **PTB2** and **PTB6** systems as examples to illustrate this point. Figure 6 shows the CAFM current images at fixed bias voltage of −2 V for films **PTB2**/PC$_{61}$BM and **PTB6**/PC$_{61}$BM. Consistent with TEM study, we observe donor/acceptor interfaces throughout the films with interpenetrating networks of donor/acceptor material in the **PTB2** film. The high hole current features (dark areas) are contributions from polymer-rich domains and are distributed uniformly over the whole **PTB2**/PC$_{61}$BM film surface, which makes the solar cells high-current

density. In contrast, there are low-current areas in the images and largely phase-separated features throughout the **PTB6**/PC$_{61}$BM films. The much lower current (see the difference in scale bar) of **PTB6** reflects the lower hole mobility of **PTB6** than **PTB2**.

This morphological problem can be remedied by using mixed solvents in preparing polymer/fullerides spin-coating solution.[20] Primary study showed that the **PTB3**/PC$_{61}$BM blend film exhibited improved morphology by using dichrolobenzene/1,8-diiooctane (97/3, v/v) as solvent: there are no large features, and it shows similar morphology to **PTB1** or **PTB2** blend film in the TEM image (Figure 5g). The PCE of such polymer solar cell reaches 5.85%. Similar morphology change for **PTB4**/PC$_{61}$BM and **PTB5**/PC$_{61}$BM blend films was observed (Figure 5h and i). Dramatic enhancement in solar cell performance can be observed both in **PTB4** and **PTB5** solar cells. (Figure 7a) Besides the increase of the V_{oc}, the **PTB4** solar cell shows larger J_{sc} than the **PTB5** one, possibly due to the higher hole mobility in fluorinated **PTB4**. It can also explain the slight increase of the FF in the **PTB4** solar cell. Therefore, we have successfully improved the V_{oc} from 0.58 to 0.74 V (∼28%) over the **PTB1** polymer system without scarification in photocurrent. The PCE from the **PTB4**/PC$_{61}$BM solar cell reached 5.9%. Figure 7b shows the EQE spectrum of the **PTB4**/PC$_{61}$BM solar cell prepared from mixed solvent. It can very efficiently harvest the light in the maximum photon flux region (680 nm), showing

(19) (a) Coeffey, D. C.; Reid, O. G.; Rodovsky, D. B.; Bartholomew, G. P.; Ginger, D. S. *Nano. Lett.* **2007**, *7*, 738. (b) Dante, M.; Peet, J.; Nguyen, T.-Q. *J.Phys. Chem. C* **2008**, *112*, 7241. (c) Douhéret, O.; Lutsen, L.; Swinnen, A.; Breselge, M.; Vandewal, K.; Goris, L.; Manca, J. *Appl. Phys. Lett.* **2006**, *89*, 032107. (d) Leever, B. J.; Durstock, M. F.; Irwin, M. D.; Hains, A. W.; Marks, T. J.; Pingree, L. S. C.; Hersam, M. C. *Appl. Phys. Lett.* **2008**, *92*, 013302.

(20) Lee, J. K.; Ma, W. L.; Brabec, C. J.; Yuen, J.; Moon, J. S.; Kim, J. Y.; Lee, K.; Bazan, G. C.; Heeger, A. J. *J. Am. Chem. Soc.* **2008**, *130*, 3619.
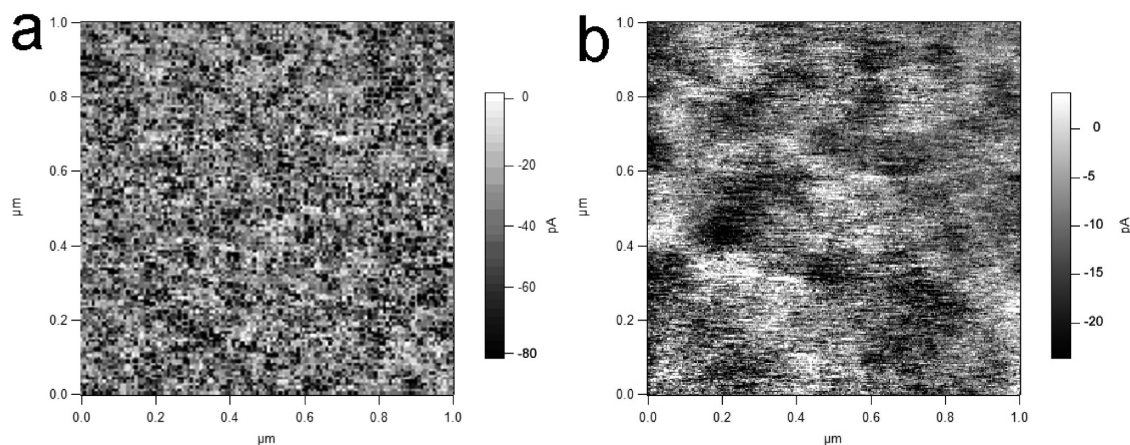
Figure 6. CAFM images of polymer/PC$_{61}$BM blend films: **PTB2** (a) and **PTB6** (b). The white regions in CAFM (low-current) correspond to the PCBM-rich areas, consistent with hole current images.
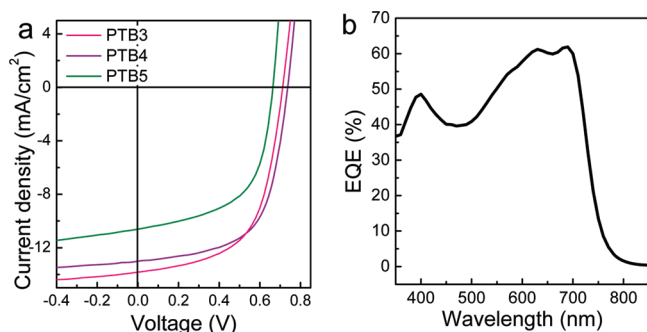

Figure 7. (a) Current−voltage characteristics of polymer/PC$_{61}$BM solar cells prepared from mixed solvents dichlorobenzene/diiodooctane (97/3, v/v) under AM 1.5 condition (100 mW/cm^2). (b) External quantum efficiency of the **PTB4**/PC$_{61}$BM device prepared from mixed solvents.

over 50% from 550 to 750 nm. A spectral mismatch factor (*M*) of 0.965 can be calculated by inserting AM 1.5 G standard spectrum, Oriel solar simulator (with 1.5 G filter) spectrum, and EQE data.[21] The efficiency of **PTB4**/PC$_{61}$BM solar cell thus reaches 6.1%, which is the highest value so far for single-layer polymer solar cells.

The shape of the EQE spectrum suggests that further improvement in PCE can be achieved by using PC$_{70}$BM in place of PC$_{60}$BM, as shown in our previous work.[8] However, primary results are not conclusive, and the performance of composite prepared with PC$_{70}$BM is inferior to those from PC$_{60}$BM. It is likely that the phase separation behavior of the polymer/PC$_{70}$BM

is different from that of polymer/PC$_{60}$BM. We are working on the optimization of the polymer/PC$_{70}$BM solar cells, and the results will be reported later.

Conclusion

A series of new semiconducting polymers with alternating thieno[3,4-*b*]thiophene and benzodithiophene units was synthesized. It was found that the physical properties of these polymers can be finely tuned for photovoltaic application. The HOMO energy levels of the polymer were lowered by substituting alkoxy side chains to the less electron-donating alkyl chains in **PTB3** or introducing electron-withdrawing fluorine into the polymer backbone in **PTB4**, leading to significant increase in V_{oc} (28%) for polymer solar cells. The side chains and substitute groups also affect the polymer's absorption and hole mobility, as well as the miscibility with fulleride, all influencing polymer solar cell performances. Films prepared from mixed solvent exhibit finely distributed polymer/fulleride interpenetrating network and significantly enhanced solar cell conversion efficiency. A power conversion efficiency of over 6% has been achieved in solar cells based on fluorinated **PTB4**/PC$_{61}$BM composite films prepared from mixed solvents.

(21) Shrotriya, V.; Li, G.; Yao, Y.; Moriarty, T.; Emery, K.; Yang, Y. *Adv. Funct. Mater.* **2006**, *16*, 2016.